Available online www.jocpr.com

Journal of Chemical and Pharmaceutical Research, 2018, 10(3):172-181

Research Article

ISSN : 0975-7384
CODEN(USA) : JCPRC5

Synthesis, Characterization and Electrochemical Behaviour of Novel Biologically Active and Antitumer Compound: 2-Amino-5-S-Benzyl-1, 3, 4-Thiadiazole

HA Fetouh[1*], AM Ismail[1], MO Bashier[2] and H Abdel Hamid[1]

[1]*Department of Chemistry, Alexandria University, Ibrahimia Alexandria, Egypt*
[2]*Sudanese Standards and Metrology Organization (SSMO), Khartoum, Sudan*

ABSTRACT

A novel and innovative compound, 2-amino-5-S-benzyl-1, 3, 4-thiadiazole (ABMT) was prepared from 2-amino-5-mercapto-l, 3, 4-thiadiazole (AMT); the assigned structure was based on spectral analysis. The activity of this compound showed pronounced antitumor activity that was confirmed from reversible redox characteristic and quantum chemical calculations. The computational evidence for the antitumor activity was obtained via the performed molecular modeling of ABMT using Gaussian 09 system. The optimal geometries of molecular skeleton and molecular orbital (MO) densities were visualized using the corresponding Gauss View software. The ABMT compound was simulated with TD-DFT method in polarizable continuum solvent model PCM of methylene chloride. The optimized geometry of the molecular skeleton and the molecular orbital (MO) densities were visualized. The stability of ABMT in aqueous solutions at pH 1.2, 6.8 and 7.4 simulating the body fluids: stomach, intestine and blood respectively was investigated using High Performance Liquid Chromatography (HPLC). The prepared compound is relatively stable and showed the best performance at pH 7.4.

Keywords: 2-amino-5-S-benzyl-1, 3, 4-thiadiazole (ABMT); Reversible redox; Molecular modeling; HPLC

INTRODUCTION

Thiadiazoles are widely used in pharmaceutical and medicinal chemistry [1-3]. Thiadiazole acts like the third and fourth generation *of cephalosporins* antibiotics. 1, 3, 4-thiadiazoles have anticancer, anti-inflammatory, antihypertensive, antidepressant, anticonvulsant, anti leishmanial, analgesic and antimicrobial activities [4]. Thiol and aminothiol compounds are efficient chemical radioprotectors and scavengers [5]. 1, 3, 4-thiadiazoles are susceptible to physical and chemical degradation under various conditions, due to the fragile molecular structure. Their physical properties and pharmacological effects may be altered as well as therapeutic efficiency and safety of uses may be reduced [6]. Chemical degradation of the drug may yield toxic products and it is related to functional groups in the molecular structure, hydrolysis, dehydration, photo degradation and transferring reactions. The chemical degradation may take place at low pH, most of drugs are fairly stable at the neutral pH found in the intestine but may be unstable in acidic medium. The methods of drug analysis include HPLC and ultraviolet-visible spectrophotometry. The latter method was widely used for the determination of drugs in the presence of alkali-induced degradation products or in pharmaceutical, urine samples and, also in solid dosage forms. Charge-transfer metal complexation was used for determination of drug in bulk samples and pharmaceutical dosage**.** In addition, that the oxidative coupling reactions of drug give an intense coloured product measured spectrophotometrically [7-9].

EXPERIMENTAL SECTION

Preparation of 2-Amino-5-S-Benzyl-1,3,4-Thiadiazole (ABMT)

2-Amino-5-S-benzyl-1, 3, 4- thiadiazole (ABMT) was prepared from a solution of 5-amino-2-mercapto-1,3,4-thiadiazole (AMT), Figure 1 (1.0 gm., 7.4 mmol.) in dry dimethyl formamide *(DMF)* (5 mL), anhydrous K_2CO_3 (2.04 gm.,14.8 mmol.) was added, the reaction mixture stirredfor0.5h., benzyl chloride (1.2 mL, 8.8 mmol) was added. Stirring was continued for overnight at room temperature, the reaction mixture was poured onto ice. The product separated out, it was collected by filtration, washed with water. It was crystallized from EtOH as pale yellow crystals (1.2 gm., 83% yield); m.p.150^{o}C. The chemical structure of the target compound (ABMT) was elucidated by FTIR, ^{1}H NMR,^{13}C NMR spectroscopic techniques as well as elemental analysis.

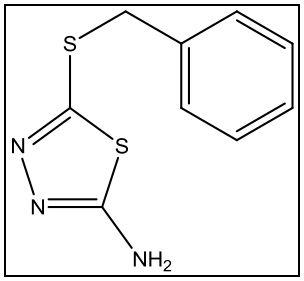

Figure 1: 2-Amino-5-S-benzyl-1, 3, 4-thiadiazole [amino mercapto benzyl thiadiazole, (ABMT)]

FTIR: 3295.23, 3104.09 (NH_2); 1615.00 (C=N); 1514.74 (C=C); 1058.21 (C-N) and 707.74 cm^{-1}(C-S).^{1}H NMR (400 MHz, *DMSO*-d_6): δ_H = 4.305 (s, 2H, S-CH_2); 7.312-7.347(m, 5H, Ar-H). ^{13}C NMR (150 MHz, DMSO-d_6): δc = 39.89 (Ph**C**H_2); 128.72; 129.09; 137.57; 149.93; 170.33 (Ar-C).
The elemental analysis of ABMT $C_9H_9N_3S_2$: (223.32 g.mol^{-1}): C, 48.30; H, 4.04; N, 18.80 is in good agreement with the found values: C, 48.40; H, 4.06; N, 18.82.

Biological and Antitumor Activity of ABMT

The biological activity of this compound was examined in Central Lab., Microbiology Department, Faculty of Science, Al-Azhar University, Cario-Egypt. Agar well-diffusion method [10] was used for investigation of antimicrobial activity of ABMT. The antifungal activity against the organisms: *Aspergillus fumigatus* (RCMB 002008) and *Candida albicans* (RCMB 05036) was studied using *amphotericin* B as a standard drug. The antibacterial activity studied against: gram positive bacteria (*Staphyllo coccus aureus* (RCMB 8010010) and *Bacillus subtilis* (RCMB 010067) using *ampicillin* as a standard drug. The gram negative bacteria used were *salmonella* SP. (RCMB 010043) and *Escherichia coli* (RCMB 010052) and *gentamycin* as a standard drug. The bacteria were cultured on nutrient agar at 30^{o}C and the funguses were cultured on sabouraud dextrose agar slopes. Briefly, 0.75 mL broth culture containing *ca.* 106 colony-forming units (CFU)/ mL strain was added to 75 mL nutrient agar medium at 45ºC, mixed well, and then poured into a 15 cm sterile metallic *Petri* plate. After solidification, 8.0 mm wells were dug with a sterile metallic borer. A solution of 1mgABMT/mL dimethyl sulfoxide *(DMSO)*) was added to respective wells *s*erved as negative control for microorganisms. Triplicate plates of each microorganism strain were prepared and incubated aerobically at 37ºC for 24 hours. The activity was determined by measuring diameter (mm) of zone showing complete inhibition with the aid of a Vernier Caliper (0.1mm precision). The growth inhibition was calculated by referring to positive control (a suitable standard specified antimicrobial drug (1 mg/mL).

Spectral Methods of Analysis of ABMT

The instrumental methods of analysis of ABMT including: a) Fourier transformer Infrared (FTIR) spectroscopy; b) Proton nuclear magnetic resonance (^{1}H NMR), ^{13}C NMR, in addition to c) HPLC and UV-visible spectroscopy. The FTIR spectrum of ABMT, was taken in KBr disc using Bruker TENSOR 37 spectrophotometer, Model 1430 covering the frequency range of 200-4000 cm^{-1}. Calibration of frequency reading was made with polystyrene film (1602 ± 1 cm^{-1}). Mp was determined with a Mel-Temp. apparatus and is uncorrected. TLC was performed on Baker-Flex silica gel 1B-F plates using ethyl acetate-petroleum ether (1:1 v/v) as eluent. The compound was detected by UV-light absorption. ^{1}HNMR spectrum was recorded on Bruker spectrometer (400 MHz) at Faculty of Pharmacy-Bani Swief University, chemical shifts (δ) are given in ppm relative to TMS as internal standard. Microanalysis was carried out at the unit of microanalyses at Cairo University.

Cyclic Voltmmetry

The redox behavior of ABMT was recorded using the cyclic Voltammetry technique. This electrochemical measurements were achieved by using three-neck electrochemical cell containing: silver/silver chloride reference electrode (RE), platinium counter electrode (CE) and graphite working electrode (WE) of the activated surface by Al_2O_3-double distilled water paste. The cell connected to Gamry potentiostate. For impedance measurement, AC signal of amplitude10 mV peak-to-peak sine wave was applied in frequency range: 0.2 Hz to 1.0×10^5 Hz with respect to the rest potential of working electrode. Five data points were taken for each frequency decade. The potentiostat controlled potential between WE and RE and measure the current response. The frequency generator provides the periodic excitation potential signal and frequency response analyzer contains all necessary electrical hardware controlled by personal computer for running the software that coordinates the execution of the experiment, data logging, and provide graphical the complex impedance spectra. Gamry instrument reference 600 sequencer software version 6.20 and GamryEchem-analyst version 6.20were used for analysis impedance spectra (Nyquist plots). The electrode surface polished with fine emery paper of 1000 grades in both top and down direction [11]. Then sonnicated in acetone-ethanol mixture (50:50% v/v) mixture for 15 min., then sonnicated in double-distilled water for 15 min., and air dried. 50 µL 100 ppm ABMT solution was distributed on electrode surface by a micropipette and air dried for time interval from (0.5 h. to 24 h.) till complete dryness. The WE was introduced into 100 mL cell containing supporting electrolyte (60 mL of 1.0 M KCl and 40 mL phosphate buffer of pH 7.0) connected to the potentiostat in conjunction with an ultra-thermostat adjusted at 25 ± 1°C. The equilibrium potential of WE was established after 15 min. when potential variation is 1.0 mV/ min. to ensure reliable measurements.

RESULTS AND DISCUSSION

Biological Activities of 2-Amino-5-S-Benzyl-1,3,4-Thiadiazole

ABMT showed potent *antifungus* activity only against *Candida albicans* and the best antibacterial activity for *Salmonella SP* (Table 1). The biological in diffusion agar technique, well diameter: 6.0 mm (100 µL was tested), RCMB: Regional Center for Mycology and Biotechnology. Figure 2 and Table 2 showed that ABMT showed highly potent cytotoxic effects against A-549 cell lines which indicated excellent antitumor properties for lung carcinoma, and good cytotoxic effects against different cell lines as HepG-2 (liver carcinoma), CACO-2 (intestine carcinoma),. The ABMT showed relatively low cytotoxic effects against the RD cell line (muscle carcinoma). The IC_{50} of AMBT approached that of the standard drugs in case of Lung carcinoma. This finding indicated the best performance of ABMT in Lung carcinoma.

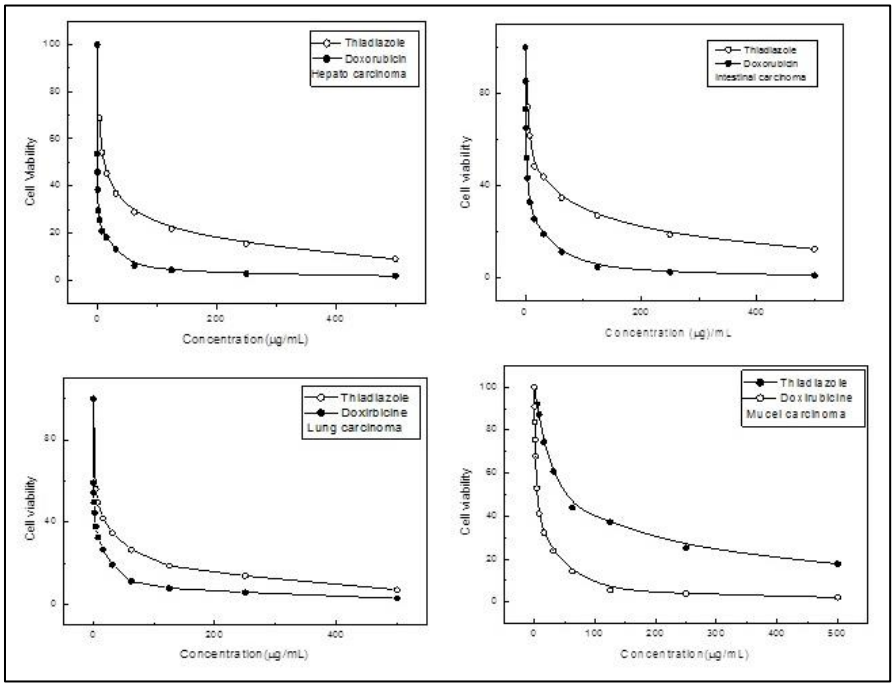

Figure 2: Relation between cell viability and concentration for ABMT and doxirubicin for various types of carcinoma

Table 1: The inhibition zone of *antimicrobial* activity of ABMT

Microorganism	Inhibition Zone	Standard drug (Control)	Inhibition Zone
Fungi			
Aspergillusfumigatus (RCMB 002008)	NA	*Amphotericin B*	23
Candida albicans (RCMB 05036)		*Amphotericin B*	25
Gram positive bacteria			
(*Staphyllococcusaureus* (RCMB 8010010)	12	*Ampicillin*	23
Bacillus subtilis (RCMB 010067)	14	*Ampicillin*	32
Gram negative bacteria			
Salmonella SP. (RCMB 010043)	15	*Gentamycin*	17
Escherichia coli (RCMB 010052)	13	*Gentamycin*	19

NA refers no activity

Table 2: The percentage of cell viability and concentration, activity of ABMT

Hepato carcinoma					**Intestinal carcinoma**		
ABMT µg/mL	**% Viability**	**Dox. µg/mL**	**% Viability**	**ABMT**	**% Viability**	**Dox. µg/mL**	**% Viability**
500	8.89	500	1.72	500	12.41	500	0.89
250	15.43	250	2.7	250	18.58	250	2.44
125	21.78	125	4.22	125	26.91	125	4.55
62.5	28.9	62.5	6.13	62.5	34.63	62.5	11.16
31.25	36.82	31.25	13.05	31.25	43.85	31.25	19.02
15.6	45.31	15.6	18.13	15.6	48.34	15.6	25.43
7.8	54.17	7.8	20.81	7.8	61.72	7.8	32.74
3.9	68.74	3.9	25.59	3.9	74.19	3.9	43.3
0	100	2	29.5	0	100	2	52.11
		1	38.39			1	64.94
		0.5	45.84			0.5	73.2
		0.25	53.57			0.25	85.33
		0	100			0	100
IC_{50} (µg/mL)							
11.5		0.36		14.6		1.93	
Lung carcinoma					**Muscle carcinoma**		
ABMT µg/mL	**% Viability**	**Dox. µg/mL**	**% Viability**	**ABMT**	**% Viability**	**Dox. µg/mL**	**% Viability**
500	7.25	500	2.98	500	17.83	500	2.2
250	13.89	250	5.94	250	25.36	250	4.02
125	18.74	125	7.94	125	37.28	125	5.55
62.5	26.59	62.5	11.28	62.5	43.95	62.5	14.35
31.25	34.81	31.25	19.39	31.25	60.72	31.25	24.02
15.6	41.92	15.6	26.74	15.6	74.51	15.6	32.37
7.8	49.56	7.8	32.55	7.8	87.29	7.8	41.11
3.9	56.13	3.9	37.94	3.9	92.06	3.9	52.94
0	100	2	44.67	0	100	2	67.93
		1	49.59			1	75.48
		0.5	54.25			0.5	83.67
		0.25	59.14			0.25	90.97
		0	100			0	100
IC_{50} (µg/mL)							
7.54		0.95		51.2		4.8	
500	13.65			500	10.43		
250	20.74			250	18.72		
125	31.49			125	26.15		
62.5	38.79			62.5	34.96		
31.25	46.21			31.25	45.18		
15.6	58.16			15.6	60.94		
7.8	72.34			7.8	78.75		
3.9	87.25			3.9	91.82		
0	100			0	100		
IC_{50} (µg/mL)							
26.3				17.4			

Electrochemical Behaviour of ABMT

The redox characteristic of ABMT was clarified *via* reversible cyclic voltamogram shown in Figure 3 indicating that ABMT is reversibly reduced on cathodic polarization and oxidized on anodic polarization. This finding confirms its anticancer activity by donating of the lone pair of electrons to free radical species in the tumor cell. The reversibility of cyclic voltamogram indicated that ABMT can be regenerated after oxidation in the human body. The ABMT exhibited a signal reversible electrochemical wave over the examined potential range with the oxidation potential of ABMT, $E_{1/2}$ = 0.38 V confirmed the purity of ABMT [12].

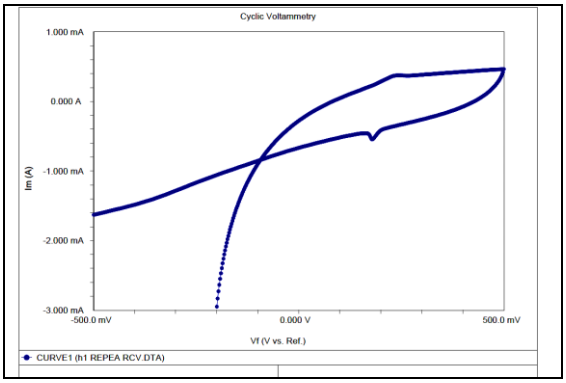

Figure 3: Cyclic voltamogram of ABMT loaded on the activated graphite electrode

Molecular Modeling of 2-Amino-5-S-Benzyl-1,3,4-Thiadiazole (ABMT)

Molecular modeling and calculation were carried out at the DFT level (B_3LYP) and 3-21G basis set and Polarizable Continuum solvent Model PCM and considering nucleus and electrons constitute the atoms as point charges with an associated mass and interactions between neighboring atoms described by elastic chemical bonds and Vander walls forces. Figure 4 showed the optimized chemical structure of ABMT and Table 3, clarified the bond lengths, bond angles, Mulliken charges and the dihedral angles. The compound contains 23 atoms, 116 electrons with stoichiometric formula ($C_9H_9N_3S_2$) and it is electrically neutral.

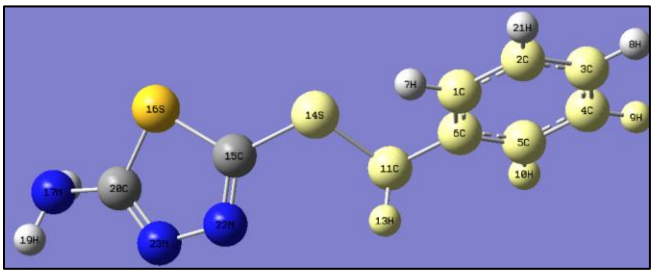

Figure 4: Molecular modeling of ABMT

All C-H atoms are of bond length nearly 1.1 Å, and most C-C atoms in the phenyl group are of the same bond length of nearly 1.4 Å, The C-N bond length (1.38 Å) is shorter than C-C bond due to electronegative character of N atoms. The bond angles are around 120° and 109.5° are attributed to triagonal planar: sp^2 and tetrahedral: sp^3 hybridization of atoms. Some dihedral angles lie in the range of (179°) or (-179°) due to distortion in linearity of sp^3 hybridization. However, dihedral angles in the range of (120.0°) or (-120.0°) were due to deviation from sp^2 hybridization. The dihedral angles proved near planarity of ABMT molecule, where angles were of nearly 180°C and 0°C. The difference was due to syn and anti positions of atoms gave 0°C 180°C respectively. The negative charge is located on S(16), S (14), while the positive charges on N(22), N(23) indicated that S is the donor center in the molecule and so most of configurations have sp^2-hybridization, and dihedral angles are 179±1º, where distribution of atoms are in the same plane. The bond length N(23)-H(51) and N(23)-H(52) leading to 1.054 Å. Also, there is a similarity in bond length of most of C-H bonds, replacement of carbon atoms by nitrogen (H-N) decreased bond length, due to the more electronegative character of nitrogen atoms. Some of dihedral angles lie in the range of (152.5°) - (-179.0°), referred to distortion in the linearity of sp^3 hybridization. However, dihedral angles varied in the range of (133.0°) -(-138.5°) due to deviation from sp^2 hybridization, while dihedral angles range from (60.4°) - (-62.5°) pointed to strong deviation from perpendicular angle, which attributed to distortion effect. The negative charge is located on S (14), S (16) indicated that S is the donor atom of lone pairs of electrons to any acceptor [12].

Dipole moment (field-independent basis) along x, y, and z axis (μ_x equals 1.5454, μ_y: -2.0290 and μ_z: 0.8784. Total dipole moment equals 2.6975 Debye indicate that the separation of charge in ABMT molecule and its ability to act either as Bronsted acid or Lewis acid. Figure 5 represents the zoom out region of molecular orbitals of the electronic distribution in ABMT molecule. According to Frontier Molecular Orbital Theory (FMO) of chemical reactivity, electron transfer occurs from (highest occupied molecular orbital HOMO of ABMT into (lowest unoccupied molecular orbital) LUMO of reactant [12]. The energy of HOMO is directly related to ionization potential. High E_{HOMO} indicates a tendency of molecule to donate electrons to appropriate center molecules with low energy vacant orbital. Energy of LUMO directly related to electron affinity. The lower E_{LUMO} indicated the stronger electron accepting ability of ABMT through back donation after forming the coordinate bond [13].

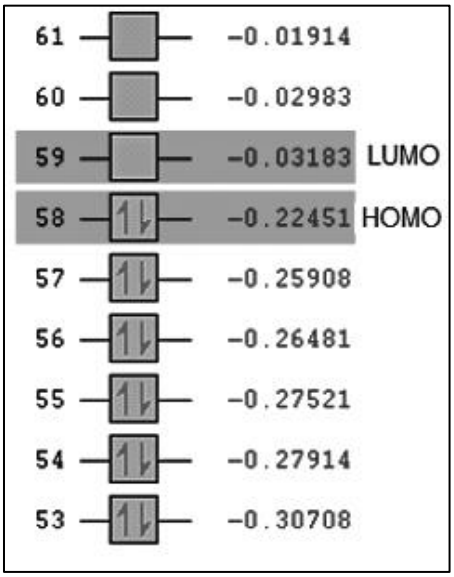

Figure 5: Energy level diagram of ABMT

The quantum chemical parameters, electron negativity, χ, chemical potential (μ_i), hardness (η)and softness (σ) were calculated from equations:

$$\mu_i = -\chi = \frac{E_{HOMO} + E_{LUMO}}{2} \quad (1)$$

$$\eta = \frac{E_{LUMO} - E_{HOMO}}{2} \quad (2)$$

$$\text{Softness, } \sigma = \frac{1}{\eta} \quad (3)$$

The ABMT has a small energy gap ($\Delta E_{LUMO-HOMO}$), so it is soft compound and can be act as Lewis acid and easily undergoes charge transfer to the free radical species in the tumor cells.

Table 3: The calculated quantum chemical parameters for ABMT

Parameter		Parameter	
E_{HOMO} (eV)	-0.22451	χ (electronegativity)	0.12777
E_{LUMO} (eV)	-0.03103	μ_i (chemical potential)	-0.12777
ΔE (eV)	0.19348	η (hardness)	0.09674
		σ (softness)	10.337

The wave function of HOMO and LUMO of ABMT lies on thiadiazole ring and on the phenyl ring (with vacant P-orbitals) respectively (Figure 6).

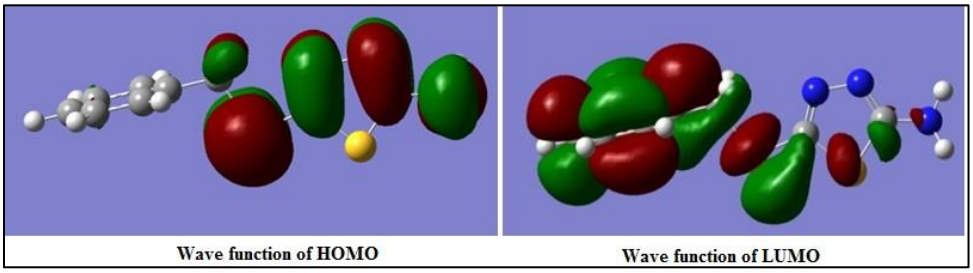

Figure 6: The location of HOMO, and LUMO orbitals in ABMT

The Chemical Stability of 2-Amino-5-S-Benzyl-1, 3, 4-Thiadiazole

The validity of HPLC method of analysis is confirmed by constructing a standard curve for a series of ABMTconcentrations dissolved in methanol. The HPLC instrument calibrated by recording the chromatogram mobile phase that remains unchanged along time of running the techniques [14].

Each concentration was injected into HPLC instrument using filtered and degassed mixture of mobile phase at flow rate 1 mL/min. Stationary phase was Column C8, the detector is a UV-visible (λ= 254 nm). Solutions of ABMT dissolved in methanol were injected into an HPLC instrument at 25^{o}C. The peak of mobile phase appeared at1.85 min. The Retention time (R_t) elapsed between sample injection and appearance at the detector. The peak of ABMT appeared at R_t from 7 to 9 min. The area under curve becomes more sharp on increasing concentrations of ABMT. The area under peak increased reached 8.8 × 10^5 mm^2 at 40 ppm ABMT. The variation of the area with the concentration of ABMT is represented in Table 4. Figure 7 showed the linear variation of area under the peak with the concentration of ABMT. On applying the least square method, a good straight line obtained with correlation coefficient approaching the unity confirming the validity of HPLC as an analytic method for ABMT. The values of LOD and LOQ were calculated using the values of the standard deviation (σ) and the slope (S) [15]. The values of LOD ($\frac{3\sigma}{S}$) and LOQ ($\frac{10\sigma}{S}$) were collected in Table 5.

Table 4: The area under peak (mm^2 × 10^5) for different concentration of ABMT in methylene chloride or methanol

Methylene chloride		Methanol	
Concentration of ABMT (ppm)	**Area under peak**	**Concentration of ABMT (ppm)**	**Area under peak**
4	125083	5	95000
6	253296	10	21000
10	438491	20	43000
16	658027	30	64000
32	1409477	40	88000

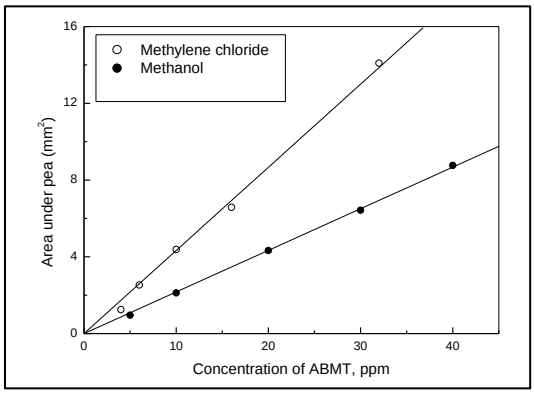

Figure 7: Standard calibration curve of ABMT in methylene chloride and Methanol

Table 5: The values of limit of detection (LOD) and limit of quantification (LOQ)

Solvent	Standard deviation (σ)	Slope (S)	Correlation coefficient	LOD	LOQ
CH_2Cl_2	0.32273	0.43322	0.99901	2.235	7.45
MeOH	0.08953	0.21687	0.99987	1.2348	4.1283

The lower values of LOD ($\frac{3\sigma}{S}$), and LOQ ($\frac{10\sigma}{S}$) (indicated that methanol is more superior solvent for the HPLC analytical method. The ABMT like similar organic compounds may undergo protonation or rearrangement of thiadiazole ring. An amorphous drug substance tend to change to more thermodynamically stable crystalline state

having low free energy, crystallization of amorphous drug substance occurs during long-term storage and may lead to drastic changes in its release characteristic, and affect its efficiency and toxicological behavior [16].

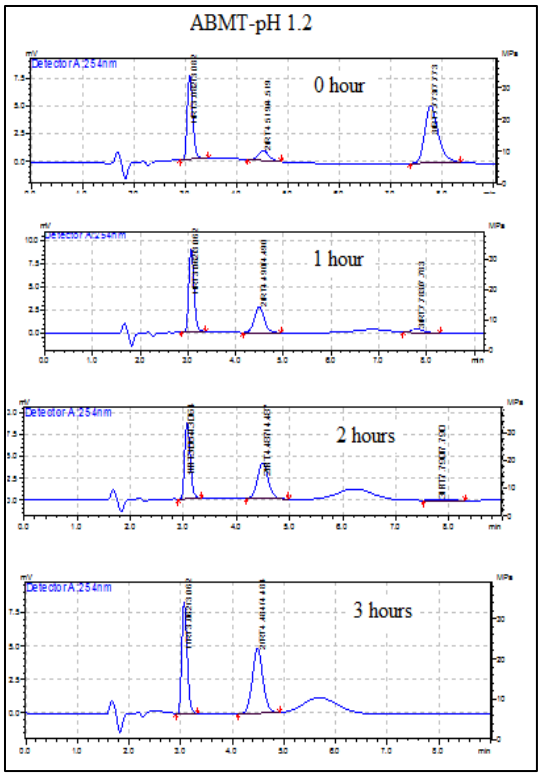

Figure 8: HPLC chromatogram for ABMT in aqueous solution at pH 1.2

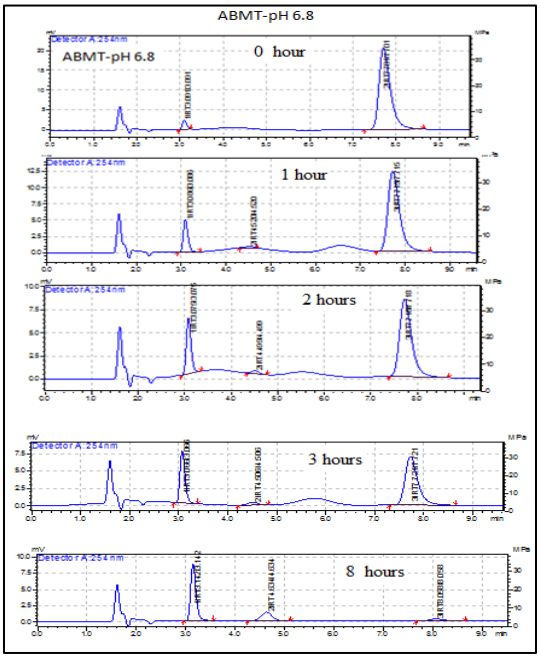

Figure 9: HPLC chromatogram for ABMT in aqueous solution at pH 6.8

The quantitation stability expresses degradation products with time of ABMT, was followed using HPLC in aqueous solutions of pH: 1.2, 6.8 and 7.4 by injection of 50µ L of 2 ppm ABMT in each aqueous solution into HPLC instrument. Figures 8-10 showed the peaks of ABMT as well as peak of mobile phase (at 1.85 min.). While, two

peaks of ABMT appeared at (R_t) 4.5, and 7.7 min. After one hour of time elapse from injection, intensity of peak at R_t 7.7 min. decreased and that of peak at (R_t) 4.5 min. increased. The data obtained are represented in Figure 11.
In all investigated solutions, area under peak at R_t 7.8 min. decreased. While area under peaks at R_t :4.5, and 3.09 min. increased along the contact time of ABMT with the aqueous solution. The rapid degradation of ABMT in acidic media through two hours may be due to protonation of nitrogen atoms in thiadiazole ring, while the at pH 6.8 and 7.4, the change in peaks may be due to rearrangements of ABMT and its conversion into its isomeric triazolinethione. This finding confirmed from matching data observed in literature for similar compounds [17]. Figure 11 showed variation of area under peaks for ABMT in aqueous solution of different values of pH.

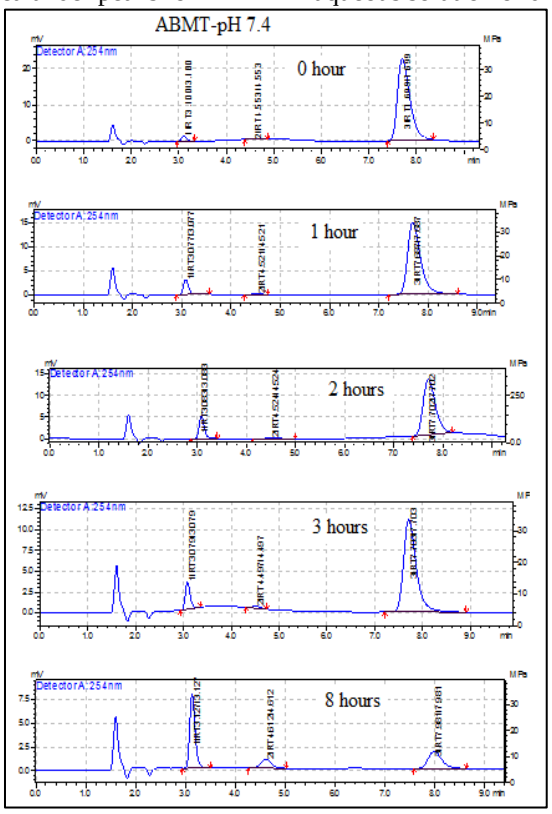

Figure 10: HPLC chromatogram for ABMT in aqueous solution at pH 7.4

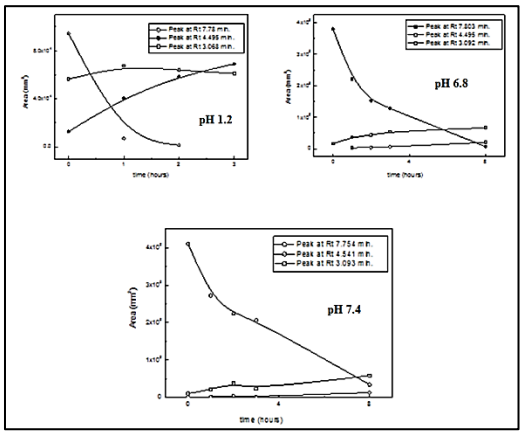

Figure 11: Variation of the area under peaks for ABMT in aqueous solution of pH (1.2, 6.8, and 7.4).

The ABMT is more stable in near neutral aqueous solutions of (pH 6.8 and 7.4) as reflected in prolonged time up to 8.0 hours in both cases.

CONCLUSION

The current work provides a novel drug: 2-amino-5-S-benzyl-1, 3, 4- thiadiazole (ABMT) which is a promising biologically active compound and can be used as an anticancer drug for many types of carcinoma as evident from study of biological activity, cyclic voltammetry and quantum chemical calculations. The compound showed the highest relative stability in the slightly alkaline medium (pH 7.4).

REFERENCES

[1] SM Gomha; TA Salaheldin; HM Hassaneen; HM Abdel-Aziz; MA Khedr. *Molecules*. **2015**, 22, 21(1), 3.
[2] SM Gomha; FM Abdelrazek; AH Abdelrahman; P Metz. *Heterocycles*. **2016**, 92(5), 954-967.
[3] SM Gomha; MM Edrees; F Altalbawy. *Int J Mol Sci*. **2016**, 17(9), 1499.
[4] S Haider; MS Alam; H Hamid. *Eur J Med Chem*. **2015**, 92, 156-177.
[5] C Prouillac; P Vicendo; JC Garrigues; R Poteau; G Rima. *Free Radical Bio Med*. **2009**, 46(8), 1139-1148.
[6] K Tripathi. Essentials of medical pharmacology. JP Medical Ltd, Jaypee High Lights Medical Publishers Inc., India, **2013**.
[7] AH Beckett, JB Stenlake. Practical Pharmaceutical Chemistry: Part II Fourth Edition, A&C Black, London, United Kingdom, **1988**, 2.
[8] S Behera; S Ghanty; F Ahmad; S Santra; S Banerjee. *J Anal Bioanal Techniques*. **2012**, 3(6), 151-157.
[9] CV Patel; AP Khandhar; AD Captain; KT Patel. *Eurasian J Anal Chem*. **2007**, 2(3), 159-171.
[10] L Boyanova; G Gergova; R Nikolov; S Derejian; E Lazarova; N Katsarov; I Mitov; Z Krastev. *J Med Microbiol*. **2005**, 54(5), 481-483.
[11] HA Fetouh; TM Abdel-Fattah; MS El-Tantawy. *Int J Electrochem Sci*. **2014**, 9, 1565-1582.
[12] M Lebrini; M Lagrenee; H Vezin; L Gengembre; F Bentiss. *Corros Sci*. **2005**, 47(2), 485-505.
[13] E Bundgaard; FC Krebs. *Sol Energ Mat Sol C*. **2007**, 91(11), 1019-1025.
[14] CC Chan, YC Lee, H Lam, XM Zhang. Analytical method validation and instrument performance verification. John Wiley & Sons, John Wiley & Sons, New Jersey, United States, **2004**.
[15] DA Armbruster; MD Tillman; LM Hubbs. *Clin Chem*. **1994**, 40(7), 1233-1238.
[16] KA Connors, GL Amidon,VJ Stella. Chemical stability of pharmaceuticals: a handbook for pharmacists. John Wiley & Sons, New Jersey, United States, **1986**.
[17] G L'Abbé; E Vanderstede. Dimroth rearrangement of 5-hydrazino-1, 2, 3-thiadiazoles. *J Heterocyclic Chem*. **1989**, 26(6), 1811-1814.